RJC

RASĀYAN *J. Chem.*
Vol. 9 | No. 3 |531 - 543 | July - September | 2016
ISSN: 0974-1496 | e-ISSN: 0976-0083 | CODEN: RJCABP
http://www.rasayanjournal.com
http://www.rasayanjournal.co.in

STUDIES ON THE BIOACTIVE EFFECTS OF INCORPORATE SOME RARE EARTH ELEMENTS INTO BASIC GLASS MATERIALS

M. A.Sherief[1,*], A. A. Hanna[1], A. A. Elkheshen[2] and A. A. Abd El Aty[3]

[1]Department of Inorganic Chemistry, National Research Centre, 33 Elbohooth St. (Tahrir) Dokki, P.O.Box: 12622, Postal code: 11787, Giza, Egypt

[2]Department of Glass Research, National Research Centre, 33 Elbohooth St. (Tahrir) Dokki, P.O.Box: 12622, Postal code: 11787, Giza, Egypt

[3]Department of Chemistry of Natural and Microbial Products, National Research Centre, 33 Elbohooth St. (Tahrir) Dokki, P.O.Box: 12622, Postal code: 11787, Giza, Egypt,

*E-mail: marwa-nrc@hotmail.co.uk

ABSTRACT

Due to the bioactivity and the excellent properties of the rare earth elements, the effects of adding different amounts of La and Ce to the familiar base glass materials were studied. Different samples with and without rare earth elements were tested without farther calcinations. X-ray diffraction and IR spectrum were used to characterize the produced mixture where scanning and EDAX were used to study the change in the morphology by adding the rare earth elements or the immersion of the produced samples in simulated body fluid (SBF) liquid. The characterization of the samples specified the formation of some phases such as $CaCe(PO_4)_2$ and $Ca_3La(PO_4)_3$. Also, it is found that the produced powder have a nano-particle size ranging from 5 to 50 nm. On other hand, it is found that the base glass materials include rare earth elements (La and Ce) have an bioactive effects on the bacteria and the fungi

Keywords: - Rare elements, Bioactive effect, Basic glass material, bacteria, fungi

INTRODUCTION

Rare earth (RE) elements are the family of elements from La (Z =57) to Lu (Z=71) and known as lanthanides group and treated chemically as one unit. The most abundant rare earth elements are La, Sm, Ce and they have special effects such as antibacterial or imaging application. Also, they have excellent properties such as high melting point, very low solubility in water, and high refractive index, so they used successfully in other industrial applications.

Due to their resemblance to calcium, lanthanides exhibit a pronounced biological activity, as they able to replace Ca^{2+} in the structured molecules[1-3]. Among the rare earth elements, cerium has found numerous industrial applications such as catalyst, fuel additives and colored component doped in different materials such as glass and ceramic[4]. On other hand, materials incorporated with cerium has shown promising antimicrobial activities[5-8], possibly due to its ability to dissociate outer membrane of bacterial cell from cytoplasmic membrane, with no damaging cytotoxic effects or loss of bio functionality by human osteasarcus cell life(HOS cells) [9].

Since 40 years ago, Hench et al[10] introduced a new application for the glass materials whatever they are silicate or phosphate as bioactive materials. Through the literatures view points, bioactive glass base materials find wide applications according to its excellent properties towards the little solubility and their thermal stability without any side effect on the medium. Most current research focuses on improvement the bioactivity of the base glass materials. These improvements include the preparation of special glass materials or incorporated of some useful elements through the basic glass materials[11]. Due to the bioactivity effects of the rare earth elements, the present work aimed to incorporate some rare earth elements into the glass basic materials to study the effects of the produced samples on the spread of some bacterial or

microbial. This work also extend to characterize the produced phases by using the spectroscopic techniques, also the morphology of the produced samples was investigated. The effect of the rare earth dose on the antibacterial effect was studied. This is the first step and the second step is converted there materials to glass.

EXPERIMENTAL

Materials and Preparation

In this work, the basic materials of phosphate glass were used to enrich the bioactive effects of the glassy materials by incorporate some rare earth elements. The starting batch composition corresponds to the following molar formula, 50 mol. % $(NH_4)_2HPO_4$ as source of phosphate, 20mol. % $CaCO_3$, 17 mol. % K_2CO_3, 5 mol. % $MgCO_3$, 3 mol. % Al_2O_3 and 5 mol. % La^{3+} or Ce^{3+} as RCl_3 (R=La or Ce) in table-1. Six samples (1, 2, 3, 4, 5 and 6) beside the blank composition were prepared. The samples were prepared as follows: All the starting materials were introduced in $(NH_4)_2HPO_4$ solution under a continuous stirring at room temperature. The reagents were added to the phosphate solution in sequence allowing 30 min. for each one to give a chance for the complete reaction. After the last addition, the stirring of the solution was continued for 30 min. extra to complete the hydrolysis reaction. Then, 1M ammonium hydroxide was added drop wise to the mixture till a gel formation was observed through the polycondensation[12]. The produced gel was dried at 120°C for 24 hrs. No further calcinations was performed

Table-1: Chemical composition of the base glass materials

Sample No.	P_2O_5 (mol %)	CaO (mol %)	K_2O (mol %)	MgO (mol%)	Al_2O_3 (mol%)	Ce_2O_3 (mol%)	La_2O_3 (mol%)
0	55	20	17	5	3	0	0
1	50	20	17	5	3	0	5
2	50	20	17	5	3	1	4
3	50	20	17	5	3	2	3
4	50	20	17	5	3	3	2
5	50	20	17	5	3	4	1
6	50	20	17	5	3	5	0

Characterization of the samples

The prepared dried samples were characterized via different techniques to study the formed phases and their morphologies

FTIR spectra

Infrared absorption spectra (IR) were performed by the KBr disc technique using a Fourier transformer infrared spectrometer (Nexus 670 FTIR, USA) in the range 400 to 4000 cm^{-1}.

X-Ray

The X-ray diffraction (XRD) was carried out by using Brukur D8 advance diffractometer (Germany) using CuKα radiation

Scanning Electron Microscope (SEM) and Energy Dispersive X-ray (EDAX) Analysis

SEM and EDAX measurements give an indication on morphology of samples surfaces. The surfaces of prepared samples will be examined by SEM after coating with gold to overcome the effect of sample charging in the electron beam and then will be examined under the scanning electron microscope. The representative scanning electron micrographs will be selected from several images made of each specimen as a result of much visual observation and selection of each area of the specimen surfaces. E DAX measurement will be performed on the best SEM shoot.

Transmission Electron Microscope (TEM)
The morphology of produced powder and the particles size were evaluated using a transmission electron microscope (TEM)

Bioactivity measurements
To study the bioactivity, 5 g of each powder sample will be soaked in 50 ml of tris-buffered simulated body fluid (SBF) solution, which resembles the human blood plasma, at 37 °C, for 30 days. The SBF will be prepared according to the recommended process by dissolving reagent NaCl, $NaHCO_3$, KCl, $K_2HPO_4.3H_2O$, $MgCl_2.6H_2O$, $CaCl_2$ and Na_2SO_4 into deionized water table 2. The solution is buffered to pH 7.4 with tris-(hydroxyl methyl)-amino methane [$(CH_2OH)_3CNH_3$] and hydrochloric acid. The immersed samples will be taken out after immersion in (SBF). Their surface analyses will be conducted via Fourier transmission IR (FTIR) using FTIR spectrometer, scanning electron microscope SEM to detect the formation of the hydroxyl apatite layer formed at the surface[13] during the immersion.

Table-2: Reagents for preparing the simulated body fluid (SBF)

Order	Reagent	Amount in gram
1	NaCl	7.996
2	$NaHCO_3$	0.350
3	KCl	0.224
4	$K_2HPO_4.3H_2O$	0.228
5	$MgCl_2.6H_2O$	0.305
6	1M HCl	40 ml
7	$CaCl_2$	0.278
8	Na_2SO_4	0.071
9	$(CH_2OH)_3CNH_2$	6.057

Effect on In-vitro Antibacterial and Antifungal Activities
In-vitro antimicrobial activities
For the determination of the antifungal properties, the produced powder samples (0, 1, 2, 3, 4, 5 and 6) were screened *in vitro* against a panel of pathogenic fungi by the agar diffusion technique in Petri dishes[14]. The produced samples containing different ratios of (La &Ce) were tested against, *Aspergillusniger* NRRL-363, *Fusariumsolani* NRC15, *Fusariumoxysporium* NRC23, *Alternariaalternata* NRC43 and *Alternariatenuissima* KM651985. All microorganisms used were obtained from the culture collection of the Department of Chemistry of Natural and Microbial Products, National Research Centre (NRC), Cairo, Egypt. The microorganisms were passages at least twice to ensure purity and viability. Agar plates were prepared by using 100 mL of suspension containing 1 $x10^6$ CFU/mL of fungi spread on potato dextrose agar (PDA). After the media had cooled and solidified, about 50 mg of the prepared powder samples were applied on the inoculated agar plates and incubated for 72 h at 28 ºC. The antimicrobial effect was evaluated by measuring the area of the inhibition halos around samples after incubation time.

RESULTS AND DISCUSSION

The interest by the base materials of glass formation because different work incorporated some RE element and using the incorporated glass in the field of the bioactive field. In this work, the different tests were carried before the formation of glass state. The produced mixtures were characterized by using different techniques:

FTIR spectra
Figure-1 represents the IR charts of the reaction mixtures with and without rare earth elements. In this study seven samples were examined representing 0, 1-5 mol. % of the rare earth elements. Also, two rare earth

elements (La^{3+} and Ce^{3+}) were added to the parent samples. The IR patterns are characterized by different absorption bands as shown in table-3. This Table exhibits the absorption bands and their assignment in the light of previous work and the literature view.

The recorded results in table-3 can be discussed as follows:

1. All the absorption bands are attributed to the phosphate based materials
2. The intensity peaks at 1006 cm^{-1} was gradually decreased by increasing the percent of rare earth elements from 0 mol. % to 5 mol.%.
3. The IR absorption band at 763 cm^{-1} is completely disappeared by adding the rare earth elements which may be explained by the improvement of the morphology of the produced samples.

Table-3: FTIR spectrum of the prepared base glass materials

The value of the absorption band (cm^{-1})	Assignment
3409	Specified HO/H produced from H_2O
2354-1643	P-OH
1432	P = O
1062 and the shoulder at 1006	asymmetric and symmetric stretching vibration of $PO3^{2-}$
883	P-O-P
763	symmetric stretching vibration in metaphosphate
566	PO_4

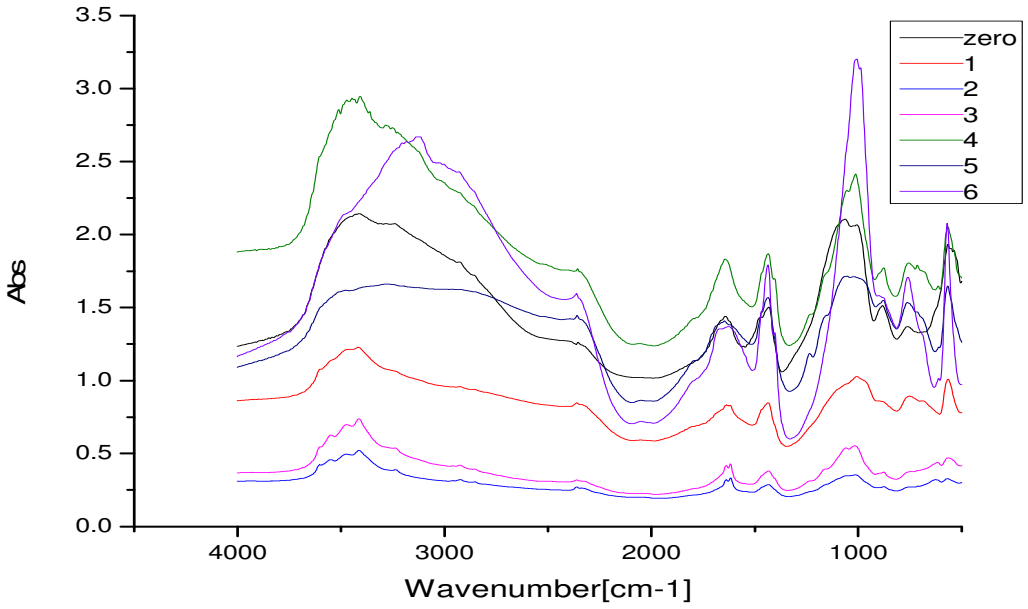

Fig.-1: FTIR spectra of the prepared samples
zero(La= 0 %,Ce= 0 %),1(La= 5%, Ce= 0 %), 2 (La= 4 %,Ce= 1 %), 3 (La= 3 %,Ce= 2 %), 4 (La= 2 %,Ce= 3%), 5 (La= 1 %,Ce= 4 %), 6 (La= 0 %,Ce= 5 %)

X-Ray

Figure-2 represents the x-ray diffraction of the mixed materials[15] without and with adding rare earth elements. The amounts of the rare earth elements are ranging from 0 to 5 % for both La and Ce. The patterns represent the x-ray chart of the as prepared samples without further calcinations, the chart of the mixture of the base glass materials including La only shows a peak at d = 3.19708 and θ = 28 which represented the

formation of $Ca_3La(PO_4)_3$ according to the card No. 29-0338. For the sample contains only Ce element, $CaCe(PO_4)_2$ is the only formed phase and the other components formed a glassy materials. It is noted that, as the percentage of Ce increases, the intensities of the specific peaks decrease, while for the predominated La element, the intensities of the specific peaks increase. This finding indicates that the presence of La element improves the crystallization of the produced phases. In all cases, the produced crystals were in nano-scale ranging from 5 to 50 nm. For the samples which contain La=3% and Ce = 2% , the x-ray patterns show two phases at d = 1.86965 and θ = 48 representing the formation of $Ca_3Ce(PO_4)_3$ according to the card No. 29-0310 and the second phase is $Ca_3La(PO_4)$ where the remainder of the base materials goes to form a glassy state dispersed as a matrix. This finding indicates that the rare earth cations can be incorporated in the base glass.

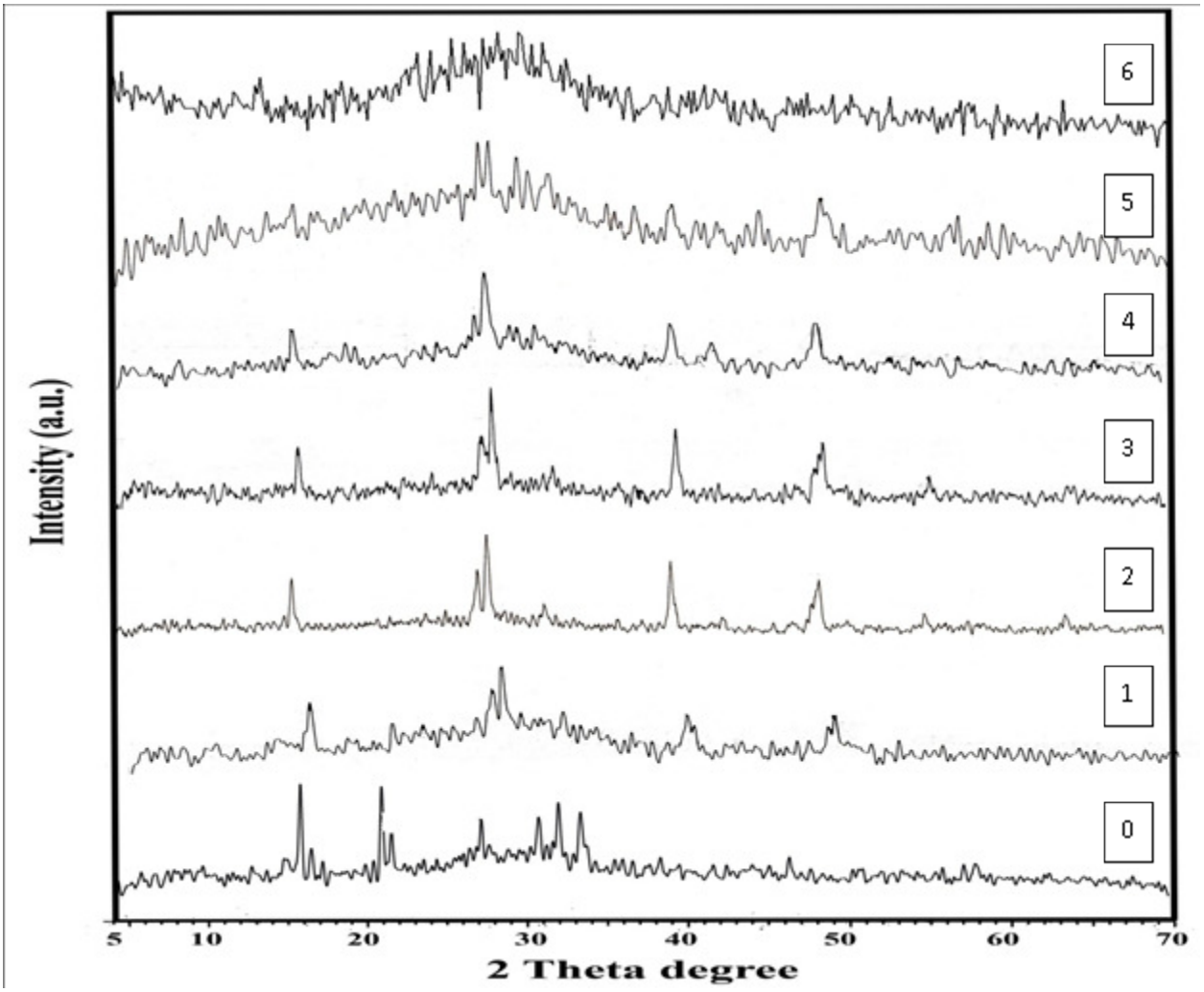

Fig.-2: X-ray of the prepared samples
Sample-0 (La= 0 %,Ce= 0 %), Sample-1(La= 5%, Ce= 0 %), Sample-2(La= 4 %,Ce= 1 %), Sample-3(La= 3 %,Ce= 2 %), Sample-4 (La= 2 %,Ce= 3%), Sample-5 (La= 1 %,Ce= 4 %), Sample-6 (La= 0 %,Ce= 5 %)

Scanning electron microscope and energy dispersive x-ray (EDAX) analyses[16]

Figure-3 exhibits the SEM in matching with EDAX of the mixture base materials and with those including rare earth elements both La and Ce. The photo of the mixture base material shows a glassy matrix[17] with some heterogeneous particles.

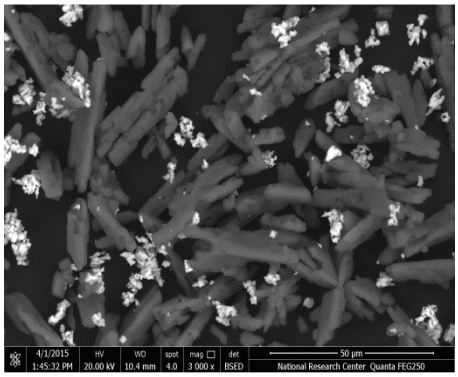

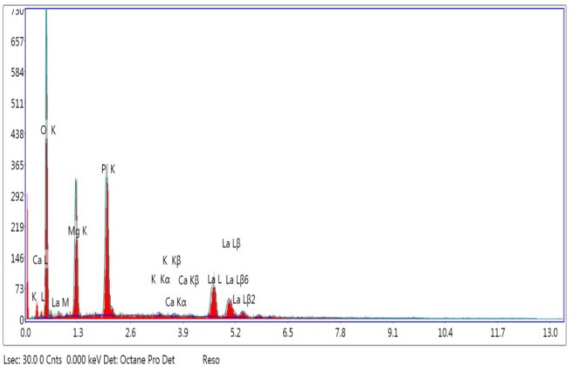

Sample-0

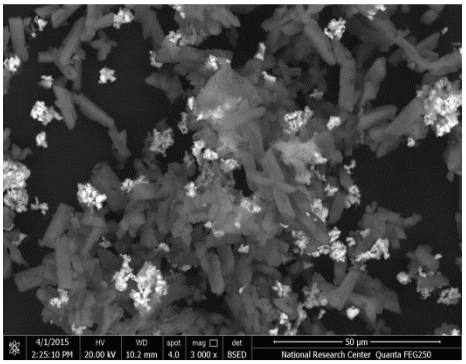

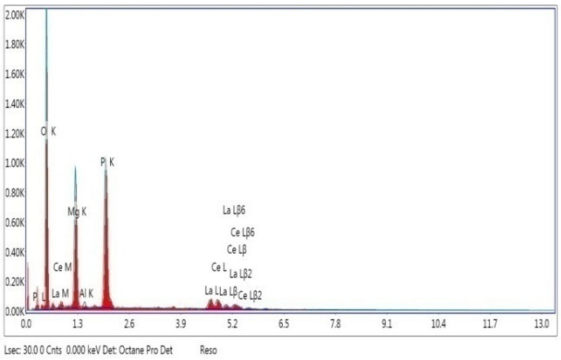

Sample-1

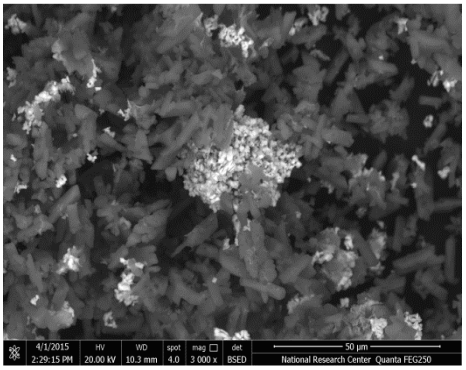

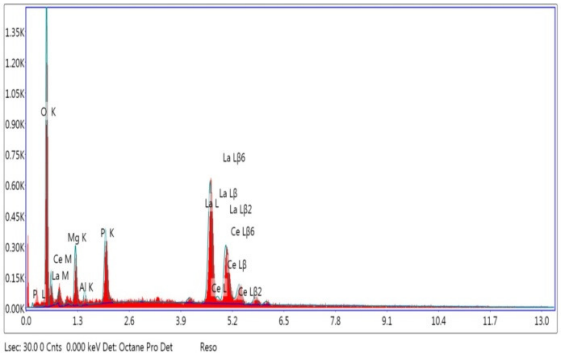

Sample-2

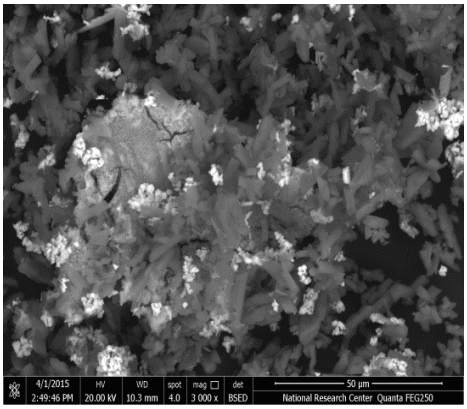

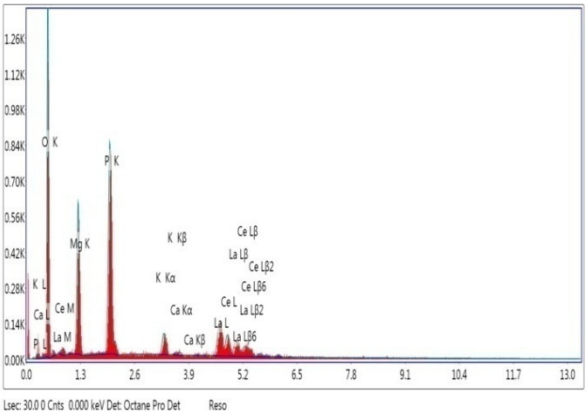

Sample-3

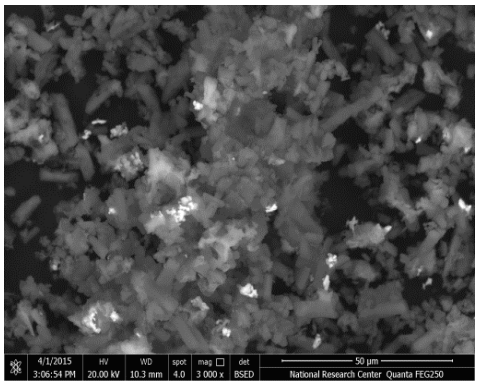

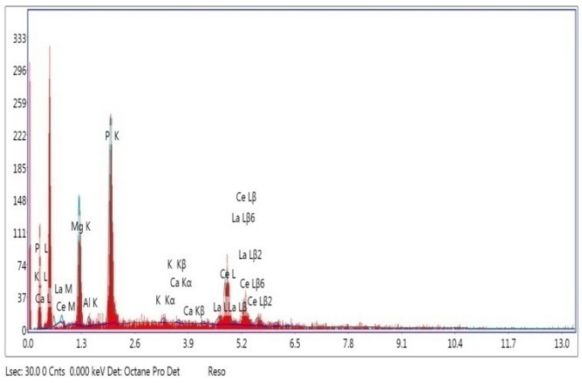

Sample-4

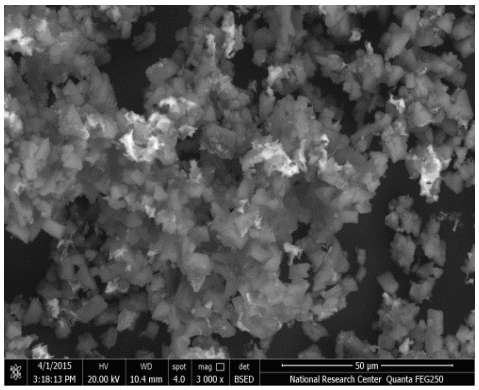

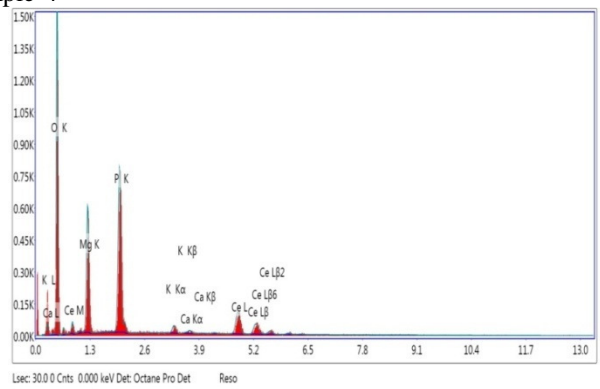

Sample-5

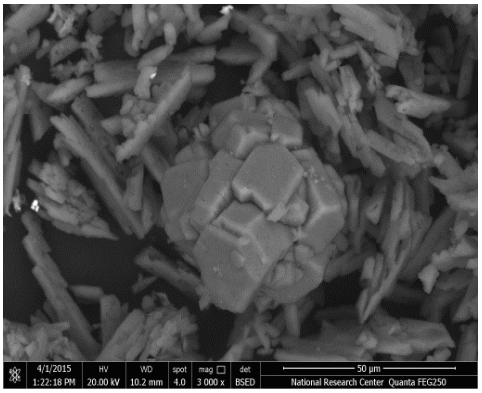

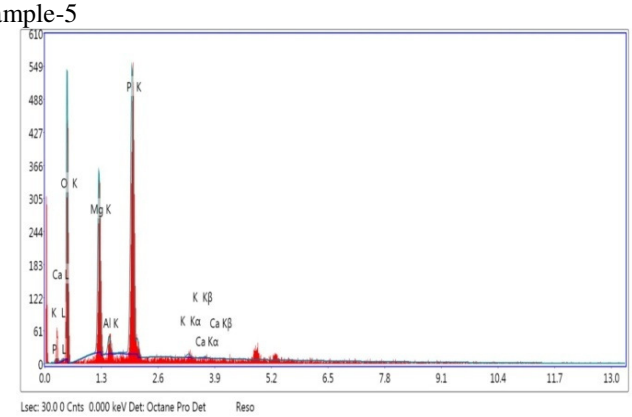

Sample 6

Fig.-3: SEM & EDEX of the prepared samples
Sample-0 (La= 0 %,Ce= 0 %), Sample-1(La= 5%, Ce= 0 %), Sample-2(La= 4 %,Ce= 1 %), Sample-3(La= 3 %,Ce= 2 %), Sample-4 (La= 2 %,Ce= 3%), Sample-5 (La= 1 %,Ce= 4 %), Sample-6 (La= 0 %,Ce= 5 %)

The particles sizes are ranging from 5 to 50 nm. As the percentage of Ce and La concentration increases, the transparency of the produced samples decreases and the surface tend to become more homogeneous and smooth with a glassy matrix. These findings are in agreement with the SEM photos of silica including La glasses [18].

Also, the results are confirmed by EDAX surface analysis Figure-3. This figure clarified the changes in the morphology of the produced phases by adding an amount of La or Ce. For the samples, the photo in matching with EDAX pattern show that the principle elements are phosphate, Mg, Ca, Al and K. These elements go to form a homogenous particle with rod shape agglomerated each other[18].

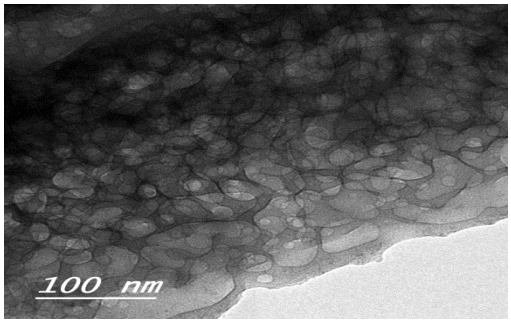

Sample-0

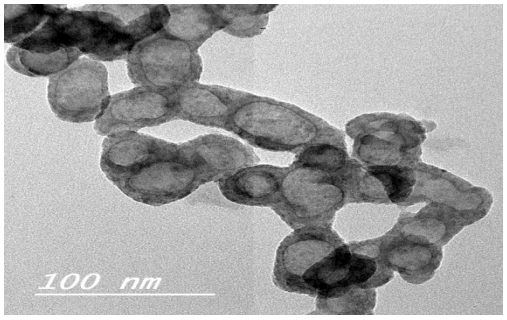

Sample-1

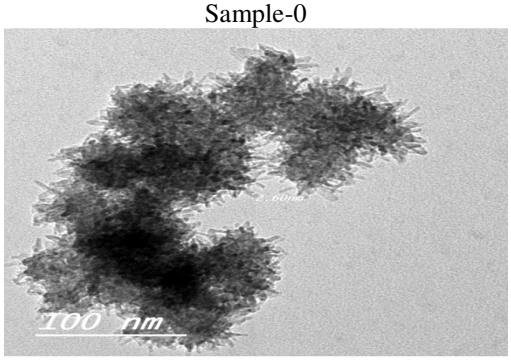

Sample-2

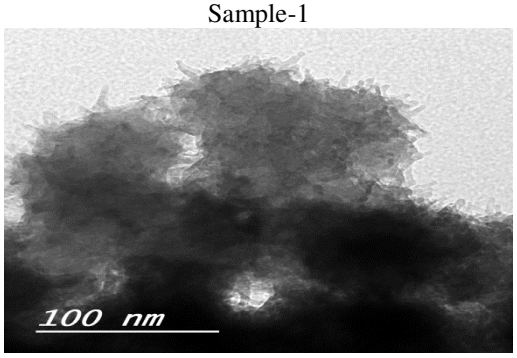

Sample-4

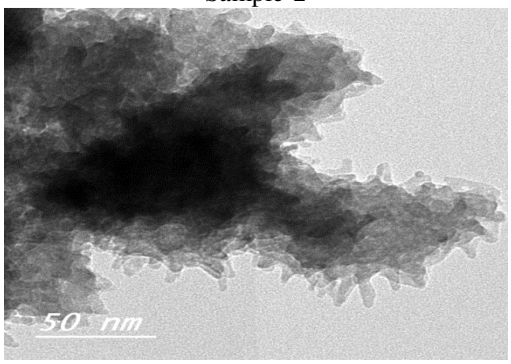

Sample-4

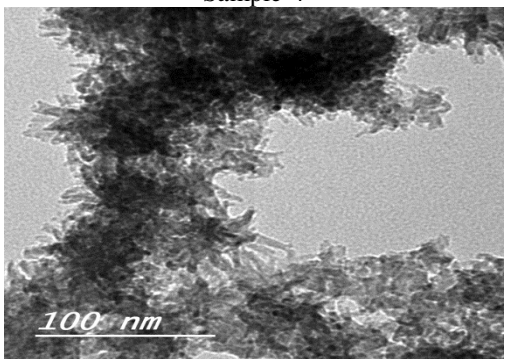

Sample-5

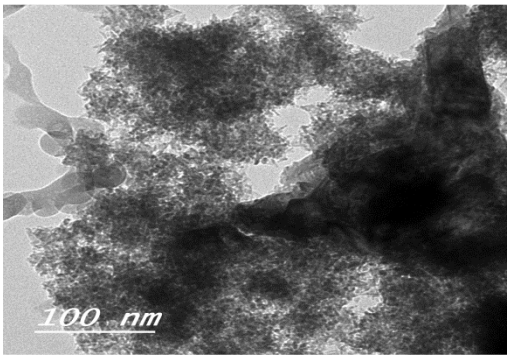

Sample-6

Fig.-4: TEM of the prepared samples

Sample-0 (La= 0 %,Ce= 0 %), Sample-1(La= 5%, Ce= 0 %), Sample-2(La= 4 %,Ce= 1 %), Sample-3(La= 3 %,Ce= 2 %), Sample-4 (La= 2 %,Ce= 3%), Sample-5 (La= 1 %,Ce= 4 %), Sample-6 (La= 0 %,Ce= 5 %)

For the photos of the other samples which included La and Ce, the EDAX exhibit the presence of both the rare earth elements owing to their percentage in the parent mixture [15]. As the Ce ions increases in the mixture, the crystallinity and the particle size decreases.

Transmission electron microscope

The TEM photos of the produced samples are represented in Figure-4, from this figure it may be concluded that as the percentage of rare earth elements increase, the formed balls tend to form irregular needle patterns.

The changes in the produced mixture were studied after immersion in the SBF solutions the results indicated that:

FTIR spectra after biological test

Figure-5 represents the IR absorption of the seven prepared samples with and without rare earth elements addition after immersion in simulated body fluid (SBF) to study the effect of this medium on the structure of the prepared samples. This study may give an indication to explain the biological behavior of the produced samples towards the formation of hydroxyapatite layer after implantation in body. The biological properties were affected by the addition of rare earth elements. From this figure, it's clear that,

1. The clearance of the bands at 565 and 602 cm^{-1} was increased by adding different amounts of rare earth elements.
2. The IR charts of the treated samples are nearly as that observed for the untreated samples. This observation indicates that no change in the structure of the samples was observed.

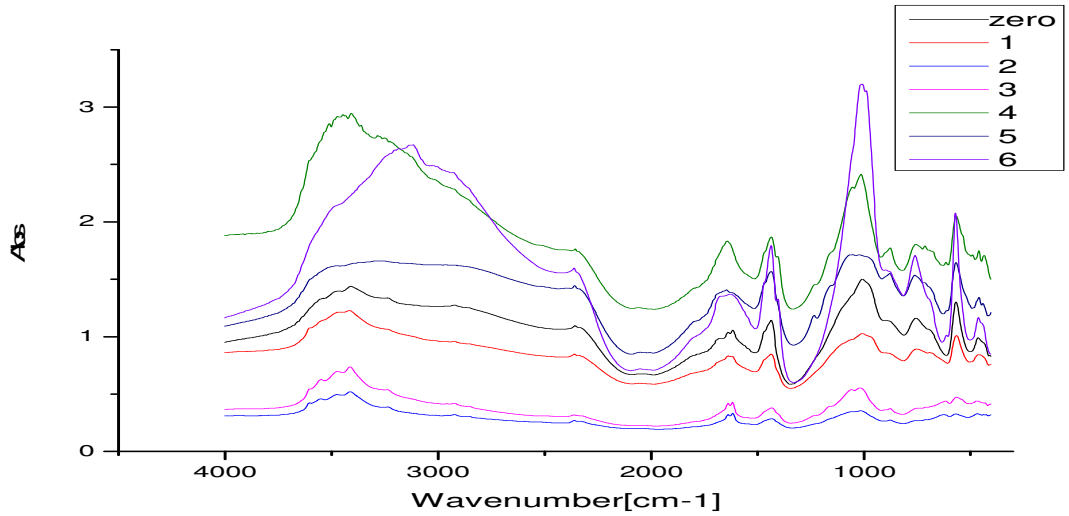

Fig.-5: FTIR spectra of prepared samples after biological test
Sample-0 (La= 0 %,Ce= 0 %), Sample-1(La= 5%, Ce= 0 %), Sample-2(La= 4 %,Ce= 1 %), Sample-3(La= 3 %,Ce= 2 %), Sample-4 (La= 2 %,Ce= 3%), Sample-5 (La= 1 %,Ce= 4 %), Sample-6 (La= 0 %,Ce= 5 %)

Scanning electron microscope after biological test

Figure-6 exhibits SEM photos of the prepared samples after soaking in SBF solution, which resembles the body plasma, for 30 days. This Figure indicates the precipitation of granules mature phase which is hydroxyapatite as shown in FTIR pattern (Figure-5). Hydroxyapatite phase (HAP) precipitation is in-vitro proving of the bioactivity of powder samples, as HAP formed layer resembles the bone structure in living organisms. It is also noticed that, the phase is not completely precipitated so, it is recommended to increase soaking period in SBF solution for enhancing the bone layer formation.

Antifungal activity

In Figure-7(a, b, c), the produced powder samples (0-6) were tested for their antifungal activity against five pathogenic fungi. The result shown in table-4 displayed that samples number (1&6) exhibited a wide range of antifungal activity against all the tested fungi compared to the other samples, with zones of inhibition range from 12 to 30 mm.

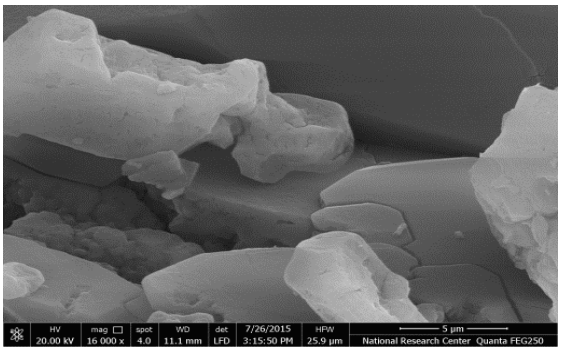

Sample-0

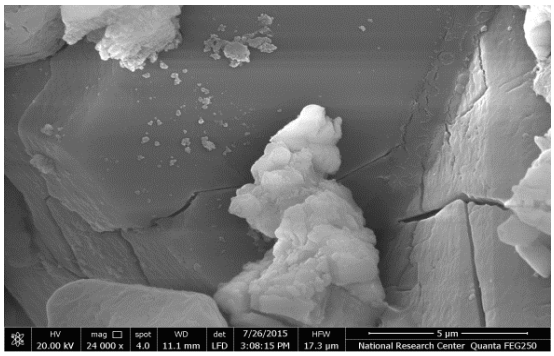

Sample-1

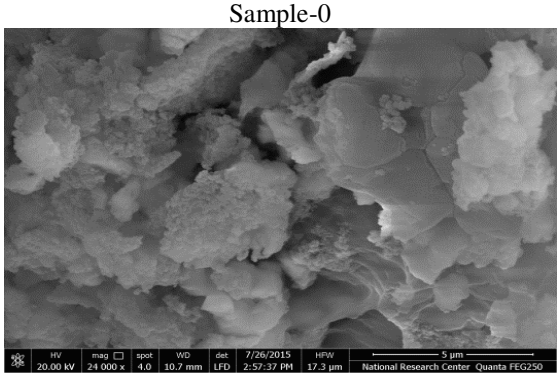

Sample-2

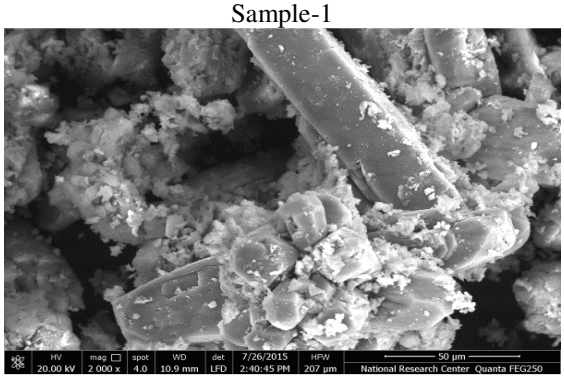

Sample-3

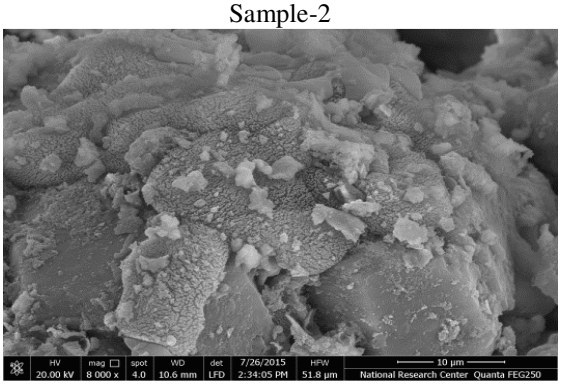

Sample-4

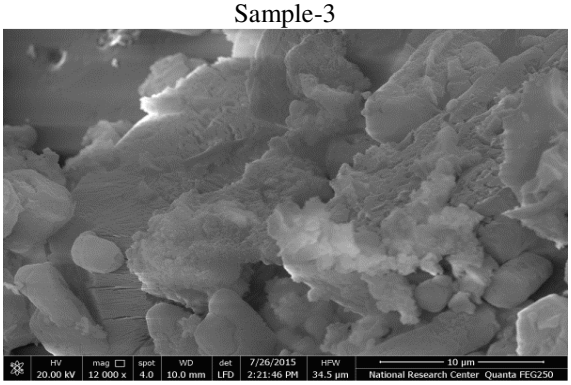

Sample-5

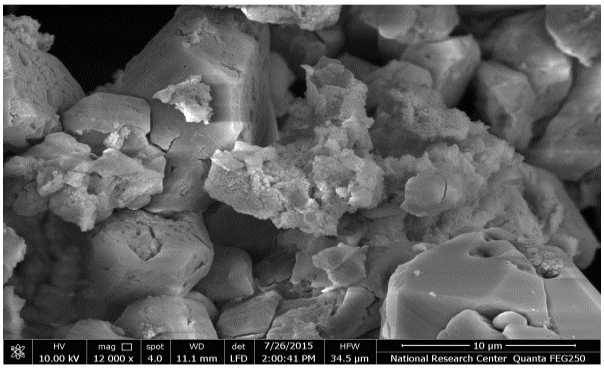

Sample-6

Fig.-6: SEM of the prepared samples after biological test

Sample-0 (La= 0 %,Ce= 0 %), Sample-1(La= 5%, Ce= 0 %), Sample-2(La= 4 %,Ce= 1 %), Sample-3(La= 3 %,Ce= 2 %), Sample-4 (La= 2 %,Ce= 3%), Sample-5 (La= 1 %,Ce= 4 %), Sample-6 (La= 0 %,Ce= 5 %)

Followed by sample number (0), (Ce= 0%, La=0%) which exhibited good inhibitory activity against A.alternata and F.solani with zones of inhibition 30 and 20 mm, respectively, and moderate activity against

A.tenuissima and A. niger with zones of inhibition 18 and 14 mm, respectively. The results also revealed that sample number (2) which contains percentage of (Ce=1% and La= 4%) exhibited antifungal activity against all tested fungi with zones of inhibition range from 15 to 25 mm except the fungal isolate F.oxysporium.

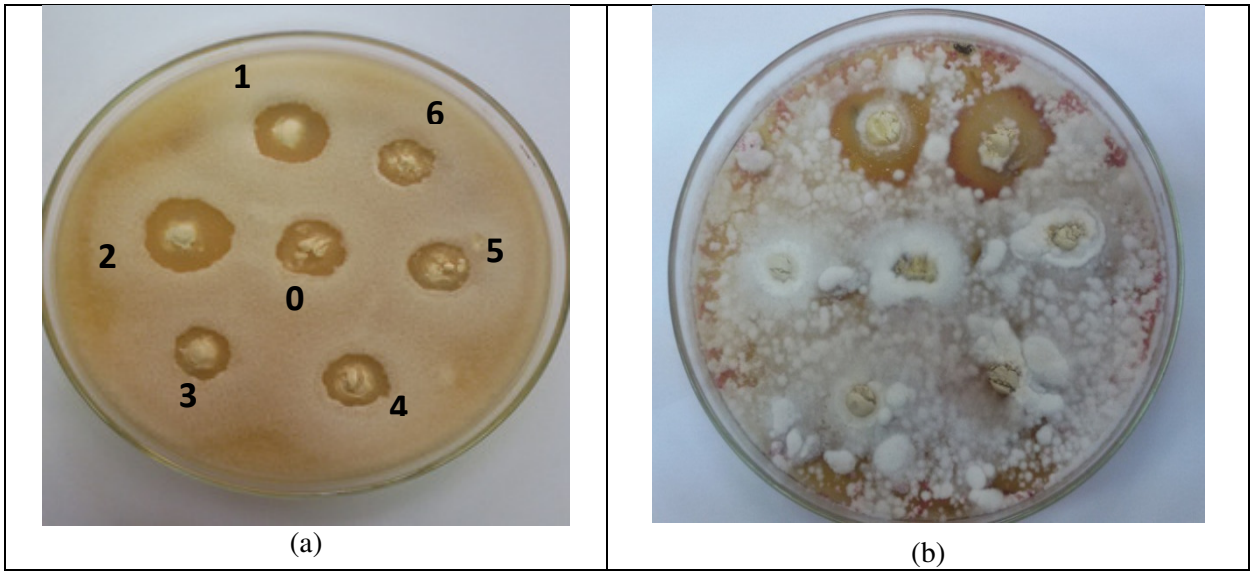

Fig.-7a: Microbiological results of agar diffusion for the prepared glass powder samples (0-6), (a) with *Fusariumsolani*, and (b) with *F.oxysporium*.
Sample-0 (La= 0 %,Ce= 0 %), Sample-1(La= 5%, Ce= 0 %), Sample-2(La= 4 %,Ce= 1 %), Sample-3(La= 3 %,Ce= 2 %), Sample-4 (La= 2 %,Ce= 3%), Sample-5 (La= 1 %,Ce= 4 %), Sample-6 (La= 0 %,Ce= 5 %)

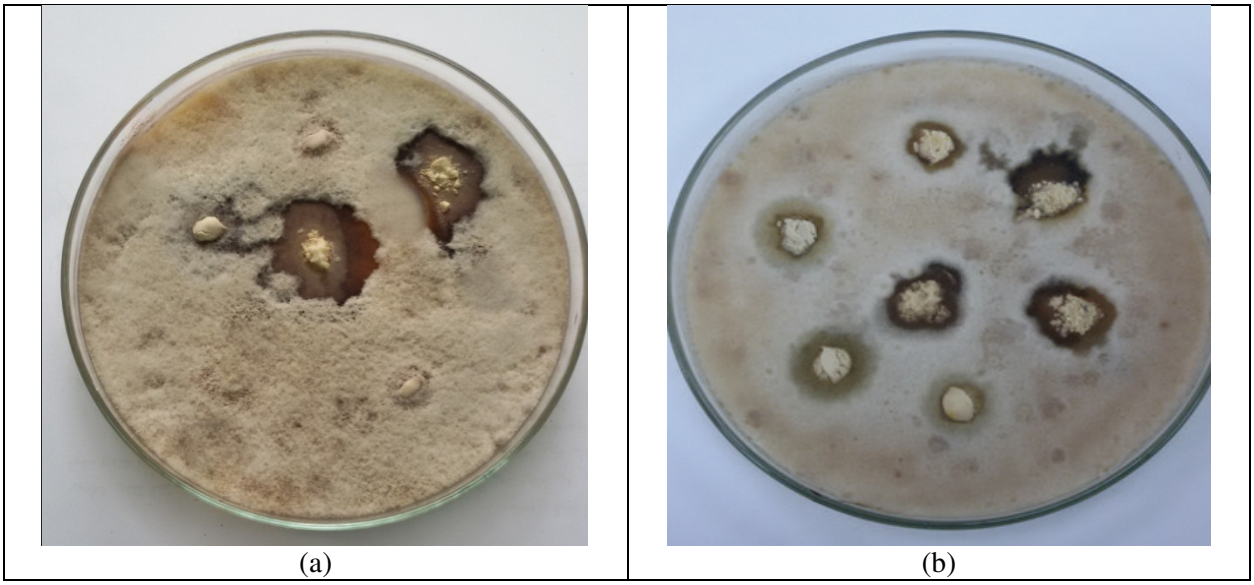

Fig.-7b: Microbiological results of agar diffusion for the prepared glass powder samples (0-6), (a) with *A.alternata*, and (b) with *A.tenuissima*.
Sample-0 (La= 0 %,Ce= 0 %), Sample-1(La= 5%, Ce= 0 %), Sample-2(La= 4 %,Ce= 1 %), Sample-3(La= 3 %,Ce= 2 %), Sample-4 (La= 2 %,Ce= 3%), Sample-5 (La= 1 %,Ce= 4 %), Sample-6 (La= 0 %,Ce= 5 %)

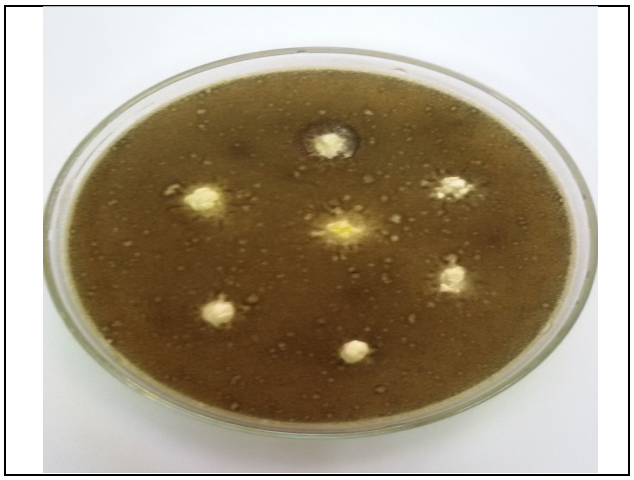

Fig.-7c: Microbiological results of agar diffusion for the prepared glass powder samples (0-6) with *A. niger.* Sample-0 (La= 0 %,Ce= 0 %), Sample-1(La= 5%, Ce= 0 %), Sample-2(La= 4 %,Ce= 1 %), Sample-3(La= 3 %,Ce= 2 %), Sample-4 (La= 2 %,Ce= 3%), Sample-5 (La= 1 %,Ce= 4 %), Sample-6 (La= 0 %,Ce= 5 %)

In addition, sample number (4) (Ce =3%, La= 2%) showed moderate inhibitory activity against *F.solani*(19 mm)and weak activity against *A.alternata, A.tenuissima* and *A. niger*, with zones of inhibition 15, 13 and 11 mm, respectively. But samples number (3&5) (Ce=2%and La=3%),(Ce=4% and La=1%) showed moderate to weak antifungal activity against *A.niger, F.solani* and *A.tenuissima* with zones of inhibition range from 11 to 18 mm and showed no activity against *F.oxysporium* and *A.alternata*[19].

(a.) Antimicrobial activity expressed as inhibition diameter zones in millimeters (mm) of the tested glass powder against the pathological strains based on the agar diffusion technique.
(b.) N.A. No activity

Table-4: Antimicrobial activity of the prepared base glass materials

Composition number	Pathogenic fungi				
	A.niger NRRL-363	*F.solani* NRC15	*F.oxysporium* NRC23	*A.alternata* NRC43	*A.tenuissima* KM651985
0	14	20	N.A.	30	18
1	12	22	25	17	15
2	15	25	N.A.	19	17
3	11	17	N.A.	N.A.	17
4	11	19	N.A.	15	13
5	13	18	N.A.	N.A.	18
6	13	17	30	25	20

CONCLUSION

From the results of this study, it may conclude that the basic glass phosphate materials incorporated with some percent of some rare earth elements without calcinations results a nano-sized particles ranging from 5 to 50 nm. Also, it is conclude that the addition of La and Ce in percent from 0 to 5% increases the bioactivity effects of the based glass materials against some kind of bacteria and fungi. So it may recommended that the conversion of the base material of glass formation resulting a glass incorporated with rare earth element and could be used as a bioactive glass.

REFERENCES

1. S.P.Fricker, *Chem. Soc. Rev.,***35(6),** 524(2006)
2. K. H. Thompson and C. Orvig, *Chem. Soc. Rev*., **35(6),** 499(2006)

3. T. C. Matsuda and M. I. Yamanaka, *Appl. Radiat lost.* **62(2),** 353(2005)
4. J. P. Garner and P.S.J.Heppell, *Burns.,* **31,**539(2005).
5. Y. Lin, Z. Yang. and J. Cheng, *J. of Rare Earths,* **25,** 452(2007)
6. X. Cai, G. J. Dai, S. Z.Tan, Y.S. Ouyang and Q.S Shi,, *Materials Letters,* **67**, 199(2012)
7. O. Zeyons, A. Thill, F. Chauvat, N. Menguy, C. Cassier- Chauvat, C. Orear, J. Daraspe, M. Auffan, J. Rose. and O. Spalla, *Nanotoxicology,***3,** 284(2009)
8. N. J. Rogers, M. N. Franklin, S. C. Apte, B. G. E.atley, B.M. Ange, J.R. Lead and M Baalousha,.*Env.Chem*.,**7**, 50(2010)
9. H. Herath, L. Di Silvio and J. Evans, *J. Biomed. Mater. Res., A***94A,** 130(2010)
10. L. L. Hench, R. J. Splinter, W.C. Allen, and T. K. Greenlee, *J. of Biomedical Mater. Res. Part A***5,** 117(1971)
11. A. Hoppe and N. S. Guldal ,A.R.Boccaccini, *Biomaterials,***32,** 2757(2011)
12. A. Bigi, E. Foresti, M. Gandolfi, M. Gazzano and N. Roveri, *J. Inorg. Biochem.,***58,**49(1995)
13. T. Kokubo In: P. Durán, J. F. Fernandez editors. Third Euro-Ceramics., Vol. 3. Castellon de la Plana: Faenza Editrice Iberica., p.1-16.(1993)
14. J. K. Domig, S. Mayrhofer, U. Zitz, C. Mair, A. Petersson, E. Amtmann, K.H. Mayer and W. Kneifel, *Int. J. Food Microbiol.*. **120,** 191(2007)
15. G. Yi-Fan, Z. A. Alshemary, A. Muhammad, A.K.R. Mohammed and H Rafaqat, *J. Cer.Intern*.,**40,** 729(2014)
16. M. Elisa, B. A. Sava, I. C. Vasiliu, R.C.C Monteiro, J. P. Veiga, L. Ghervase, I. Feraru . and R. Iordanescu., *J. of Non- crystalline Solids,* **369,** 55(2013)
17. R. C. Lucacel, A. O. Hulpus, V. Simon and I. Ardelean, *J.of Non- crystalline Solids,* **355,**425 (2009)
18. J. Coelho, N. S. Hussain, P. S. Gomes, M. P. Garcia, M. A. Lopes, M. H. Fernandes and J. D. Santos, *Current Trends on Glass and Ceramic Materials,* **87,** 115(2012)
19. O. E. Ajaiyeoba, A.P. Onocha, O.S. Nwozo and W.Sama, *Fitoterapia*.,**74** 706(2003)

[RJC-1467/2016]